Alternating Zinc Finger Motifs in the Male-Associated Protein ZFY: Defining Architectural Rules by Mutagenesis and Design of an "Aromatic Swap" Second-Site Revertant†

Michael A. Weiss*,‡,§ and Henry T. Keutmann‡

Department of Biological Chemistry and Molecular Pharmacology, Harvard Medical School, Boston, Massachusetts 02115, and Department of Medicine, Massachusetts General Hospital, Boston, Massachusetts 02114

Received May 3, 1990; Revised Manuscript Received July 11, 1990

ABSTRACT: We describe spectroscopic and biochemical studies of native and mutant Zn finger peptides from ZFY, a putative transcription factor encoded by the sex-determining region of the human Y chromosome. The parent peptide, based on ZFY domain 6, exhibits metal-dependent helix formation within a rigid tertiary framework. Nonaromatic substitutions of the consensus aromatic group (Tyr10→Ser or Lys) are surprisingly compatible with native architecture but result in loss of stability to pH or guanidine denaturation. Remarkably, these perturbations are reverted by a second-site mutation in which an alternative aromatic residue is introduced (Ser12→Phe). Design of the second-site revertant ("aromatic swap") is based on the ZFY two-finger repeat, a conserved symmetry among the ZFY-related zinc finger proteins, and is in accord with recent 2D NMR structures of Zn finger peptides. These experiments suggest general rules for metal-dependent folding of the Zn finger motif.

The Zn finger motif defines a highly conserved class of eukaryotic nucleic acid binding proteins (Klug & Rhodes, 1987; Evans & Hollenberg, 1988). A general template (Frankel & Pabo, 1988) has been proposed on the basis of sequence homologies, consisting of (i) appropriately spaced cysteine and histidine residues involved in metal coordination (Berg, 1987) and (ii) conserved hydrophobic residues apparently required for proper tertiary structure (Berg, 1988; Gibson et al., 1988). This template has been shown to define an independent unit for metal-dependent protein folding (Frankel et al., 1987) as a globular minidomain (Parraga et al., 1988; Lee et al., 1989). What is the informational content of the consensus template? Is there a canonical Zn finger, and, if so, are there specific rules that distinguish this structure from general metal-binding sites?

To address these questions, we describe comparative studies of native and mutant peptides derived from ZFY. Originally identified from studies of sex reversal in man (de la Chapelle, 1972; Page et al., 1988), this gene on the Y chromosome apparently encodes a transcription factor involved in spermatogenesis (Palmer et al., 1989; Koopman et al., 1989). Its sequence and genomic organization are similar to those of previously characterized eukaryotic transcription factors, encoding putative domains for DNA-binding and transcriptional activation (Hope & Struhl, 1986; Ma & Ptashne, 1987). The ZFY DNA-binding domain consists of 13 zinc fingers (Page et al., 1987). A homologous gene has been identified on the X chromosome of placental mammals (Schneider-Gadicke et al., 1989).

ZFY-related Zn finger proteins are distinguished from the general class of Zn finger proteins by the presence of a two-finger repeat (Page et al., 1987; Bull et al., 1988; Sinclair et al., 1988; Mardon & Page, 1989; Mardon et al., 1989; Mitchell et al., 1989; Schneider-Gadicke et al., 1989; Nagamine et al., 1990; DiLella et al., 1990). The odd-numbered domains (fingers 1, 3, 5, 7, 9, 11, and 13) fit the general Zn finger consensus sequence (Gibson et al., 1988), whereas the even-numbered domains (fingers 2, 4, 6, 8, 10, and 12) exhibit systematic differences. This alternation is strictly conserved among the ZFY-related Zn finger proteins and makes ZFY an attractive model system in which to study general features of Zn finger architecture. Indeed, pairwise alternations in finger sequence have recently been observed among a family of *Xenopus* genes related to the *Kruppel* locus (Nietfeld et al., 1989) and in a human DNA-binding protein that recognizes the enhancer element of the human immunodeficiency virus HIV-1 and a related element in the β-inteferon promoter (Maekawa et al., 1989; Fan & Maniatis, 1990). We have recently shown that odd and even ZFY domains exhibit distinguishable patterns of metal-dependent folding (Weiss et al., 1990).

In this paper the structural meaning of one alternating feature—the position of the central aromatic residue—is investigated by mutagenesis and design of a second-site revertant. Although our approach is synthetic, the language of molecular biology will be used to emphasize the genetic implications of these studies. The parent peptide is derived from ZFY domain 6 (designated ZFY-6; Figure 1A), whose structure is representative of the even subclass of ZFY-related zinc fingers. Our results demonstrate that the Zn^{2+} affinity of the *Cys*-X_2-*Cys*/*His*-X_4-*His* metal-binding motif is modulated by the stability of its tertiary structure. Within this motif the alternative aromatic positions ("aromatic swap") observed in the ZFY-related Zn finger proteins provide similar stabilizing interactions in the hydrophobic core. This study, combining mutagenesis and structural characterization, represents a first step toward defining rules for the folding and stability of the Zn finger.

Materials and Methods

Peptide Synthesis and Characterization. Peptides (Table I) were synthesized by the solid-phase procedure (Barany & Merrifield, 1979; Stewart & Young, 1984) and purified fol-

† Supported by grants from the National Institutes of Health, American Cancer Society, and the Whitaker Foundation to M.A.W. and by the Markey Charitable Trust.

* Address correspondence to this author at the Department of Biological Chemistry and Molecular Pharmacology at Harvard Medical School.

‡ Harvard Medical School.

§ Massachusetts General Hospital.

0006-2960/90/0429-9808$02.50/0

Table I: Primary Structure of ZFY-6 and Analogues[a]

Peptide	Sequence
ZFY-6	KPYQCQYCEYRSADSSNLKTHIKTKHSKEK*
	1 5 10 15 20 25
ZFY-6[Y10S]	KPYQCQYCESRSADSSNLKTHIKTKHSKEK*
	1 5 10 15 20 25
ZFY-6[Y10K]	KPYQCQYCEKRSADSSNLKTHIKTKHSKEK*
	1 5 10 15 20 25
ZFY-6[Y10K; S12F]	KPYQCQYCEKRFADSSNLKTHIKTKHSKEK*
	1 5 10 15 20 25
ZFY-6[S12F]	KPYQCQYCEYRFADSSNLKTHIKTKHSKEK*
	1 5 10 15 20 25

[a] Mutations at positions 10 and/or 12 are indicated by arrows. In each peptide a C-terminal lysine (indicated by asterisks) has been substituted for the methionine occurring at exon position 191 in the native sequence. The cysteines and histidines involved in metal binding are shown in boldface, and the conserved aromatic (Y10) and leucine (L18) are underlined.

lowing reduction (below) by reversed-phase HPLC as previously described (Weiss et al., 1990). Quantitative ninhydrin tests were used to monitor coupling efficiency, which averaged 99.1–99.3%. The following protecting groups were used on the *tert*-BOC amino acids: chlorobenzoxy (Lys), carbobenzoxy (His), bromobenzoxy (Tyr), methylbenzyl (Cys), benzyl (Ser, Thr, Glu, Asp), and tosyl (Arg).

Peptide Purification. Lyophilized, HF-cleaved peptide (75 mg) was dissolved in 0.1% acetic acid and passed over a Sephadex G-50 column and eluted with 50 mM ammonium acetate (pH 5.0). A single predominant peptide peak was eluted at a position consistent with that of a peptide monomer. The gel-filtered material was further purified following reduction (below) by reversed-phase HPLC (Beckman Gradient System 334) using a C-18 semipreparative column (Bio-Rad RP-300).

Peptide Characterization. The amino acid composition (Beckman Model 6300) and sequence (Beckman System 890) of each peptide were determined as described to verify the predicted structure. Preview analysis was performed following each step of purification as described (Tregear et al., 1977). The reduction status of cysteines (below) was confirmed following DTT treatment by reaction with iodoacetate followed by sequencing. Peptide concentration was determined by quantitative compositional analysis following acid hydrolysis.

Reduction of Cystine to Cysteine. The gel-filtered material consisted predominantly of oxidized monomers containing an intrachain disulfide. Reduction was accomplished by reaction with 0.5 M dithiothreitol in 100 mM Tris-HCl (pH 7.7 at 20 °C) at 60 °C for 1–3 h. Reduced and oxidized peptides were separated by reversed-phase HPLC using an acetonitrile gradient. Solvents were purged with argon prior to use. The reduced peptide was lyophilized and stored in vacuo.

Aggregation state was determined by gel filtration chromatography (Sephadex G-50 fine). The elution position expected for a monomeric peptide was calibrated in reference to a fragment of parathyroid hormone (residues 1–34).

Visible Absorption Spectroscopy. Metal binding of the cobalt complex was evaluated by visible absorption from 220

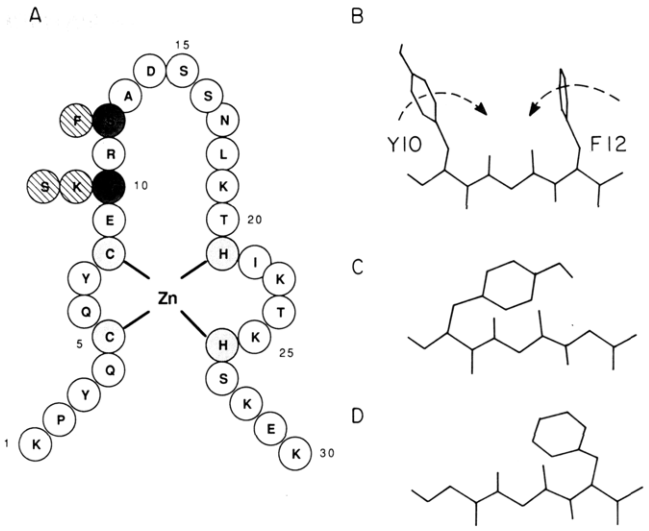

FIGURE 1: (A) Schematic representation of ZFY-6. Conserved residues involved in metal coordination (C5, C8, H21, and H26) and sites of alternative aromatic residues (Y10 and S12) are shaded; mutations at positions 10 and 12 are shown in striped circles (Table I). (B–D) Rationale for the aromatic swap experiment: in a β-strand aromatic rings at positions i or $i + 2$ (in the present case Y10 and F12) may be oriented to occupy similar positions in space.

to 800 nm as described (Frankel et al., 1987) by using a Beckman Model 15 spectrophotometer. A control solution without peptide was used as a reference. In each case 0.5 mg of reduced peptide was dissolved in 200 μL of 0.1 N acetic acid containing 15 mM cobalt chloride. The solution was brought to 1 mL by addition of 100 mM Tris-HCl (pH 8.0), providing a final concentration of 0.15 mM peptide and 0.15 mM cobalt chloride.

Circular Dichroism. CD[1] spectra were obtained by using an Aviv model spectropolarimeter. Samples were dissolved in Tris-HCl buffer (below) at a peptide concentration of 90 μM and placed in a 1 mm path length cuvette. Peptide concentrations in CD samples were determined by quantitative amino acid analysis following acid hydrolysis.

NMR Spectroscopy. Spectra were obtained at Columbia College of Physicians and Surgeons; Francis Bitter National Magnet Laboratory, MIT; NMR Facility of the University of Wiscosin, Madison; and Laboratory of Chemical Physics, National Institues of Health.

Buffers. Absorption and CD spectra were performed in 50 mM Tris-HCl (pH 7.5) containing successive aliquots of $CoCl_2$ or $ZnCl_2$. For pH titrations this buffer was mixed with aliquots of 0.1% acetic acid (containing the same concentration of $CoCl_2$ or $ZnCl_2$) to achieve intermediate pH conditions. For NMR measurements deuterated Tris-HCl was used. To delay oxidation of the peptide, buffers were purged with argon or N_2 immediately prior to use.

Results

Peptide Design and Rationale. The sequence of ZFY-6 (Figure 1A) derives from domain 6 of ZFY (residues 161–191 of the putative DNA-binding domain; Page et al., 1987). This even-numbered domain follows the consensus

(N) K - Ar Q C - Y/H C - F/Y - S/T - - - - E L - - H - - - - H S/T K

1 5 10 15 20 25

where Ar denotes an aromatic group (His, Phe, or Tyr). The

[1] Abbreviations: CD, circular dichroism; NMR, nuclear magnetic resonance.

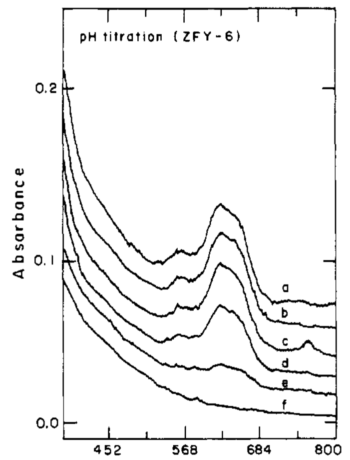

FIGURE 2: pH dependence of the visible absorbance spectrum of the ZFY-6/Co^{2+} complex: (a) pH 7.5; (b) pH 6.6; (c) pH 6.25; (d) pH 5.65; (e) pH 5.25; (f) pH 4.8.

cysteines and histidines involved in metal binding are indicated in boldface, and the conserved central aromatic residue is underlined. ZFY-6 contains a C-terminal lysine in place of methionine in the native sequence (exon position 191). This modification is included to enhance the solubility of the peptide and avoid methionine oxidation.

Design of ZYF-6 analogues was guided by general features of odd- and even-numbered domains. The odd-numbered domains are similar to the general Zn finger template (Gibson et al., 1988)

```
(N) h P Ar - C -  - C - K  - F - - - - E L - - H - - - H - A/G -
    1        5          10           15          20    25
```

where h denotes a hydrophobic residue. The odd consensus differs from that of the even (including ZFY-6) in the position of the conserved central aromatic group (F12; underlined above). To investigate the structural meaning of this difference, analogues of ZFY-6 containing mutations at positions 10 and 12 were prepared (Figure 1A). These analogues are designated according to their amino acid substitution, i.e., ZFY-6[Y10K], ZFY-6[Y10S], etc.; their sequences are shown in Table I.

In each case the reduced peptide exhibited an elution position in reversed-phase HPLC different from that of an oxidized form containing an intramolecular disulfide bond (data not shown). HPLC separation thus enabled the reduced and oxidized forms to be characterized individually and also provided an assay for inadvertant oxidation in the course of spectroscopic studies. The oligomeric state of the parent Zn^{2+}/peptide complex was evaluated by gel-filtration and found to be monomeric at the concentration and conditions of study.

Characterization of ZFY-6. The structure and metal-dependent folding of ZFY-6 are described as a baseline for comparative studies of mutant peptides (see Design of Second-Site Revertant). Atomic absorption, CD, and 1D ^1H NMR spectra provide evidence for a miniglobular domain, whose unfolding may be monitored as a function of pH and guanidine concentration.

(*a*) *Metal Binding.* The ability of reduced ZFY-6 to bind divalent metals is verified by observation of Co^{2+} thiolate charge transfer and d–d bands in the visible absorption spectrum of an equimolar Co^{2+} complex (Figure 2, spectrum a). The absence of these transitions in the presence of equimolar Zn^{2+} (not shown) reflects the greater stability of the Zn^{2+}/peptide complex; loss of charge transfer and d–d

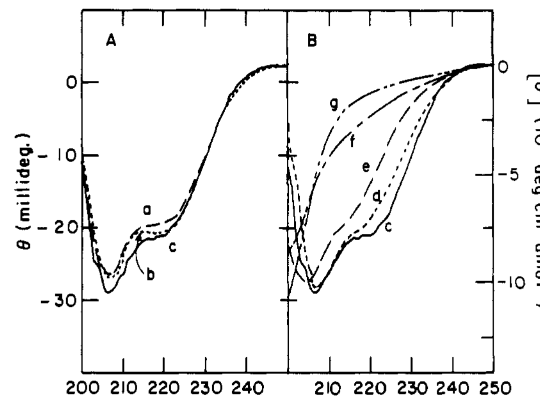

FIGURE 3: (A) Far-UV CD spectra of wild-type ZFY-6 as Zn^{2+} complex (spectrum c) and aromatic-less mutant fingers Y10K (spectrum a) and Y10S (spectrum b). (B) CD spectra of wild-type ZFY-6/Zn^{2+} complex (spectrum c), "aromatic swap" analogue [Y10K; S12F] (spectrum d), and doubly aromatic analogue S12F (spectrum e). The CD spectra of the wild-type peptide and the S12F analogue in the absence of divalent metal are labeled g and f, respectively. Normalized units (vertical axis at right) in this and the following figures are inadvertently 10% low; i.e., −10 should read −11, etc.

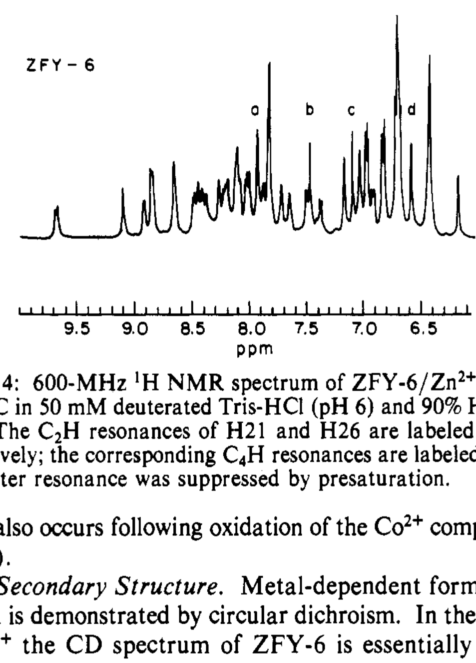

FIGURE 4: 600-MHz ^1H NMR spectrum of ZFY-6/Zn^{2+} complex at 25 °C in 50 mM deuterated Tris-HCl (pH 6) and 90% H_2O/10% D_2O. The C_2H resonances of H21 and H26 are labeled a and b, respectively; the corresponding C_4H resonances are labeled d and c. The water resonance was suppressed by presaturation.

bands also occurs following oxidation of the Co^{2+} complex (not shown).

(*b*) *Secondary Structure.* Metal-dependent formation of α-helix is demonstrated by circular dichroism. In the absence of Zn^{2+} the CD spectrum of ZFY-6 is essentially without ordered structure (spectrum g in Figure 3B); upon addition of equimolar $ZnCl_2$ a dramatic change is observed, characteristic of an α-helix (spectrum c in Figure 3B). No further changes occur at higher concentrations of Zn^{2+}, as expected for a 1:1 complex. A similar transition is observed upon addition of $CoCl_2$ (Weiss et al., 1990).

(*c*) *^1H NMR Spectroscopy.* In the absence of divalent metal the NMR spectrum of ZFY-6 resembles that of a random coil. In contrast, the 1D ^1H NMR spectrum of the Zn^{2+}/peptide complex at 600 Mhz exhibits marked dispersion of chemical shifts, reflecting a folded globular structure (Figure 4). The C_2H resonances of H21 and H26 are labeled a and b, respectively; the corresponding C_4H resonances are labeled d and c. The stability of these interactions is indicated by the observation of slowly exchanging amide resonances in D_2O for several hours (pH 6 and 30 °C; not shown). 2D NMR spectra of ZFY-6 and related analogues contain a single set of spin systems, indicating that the Zn^{2+} complex adopts a unique structure in solution. These qualitative features suggest that ZFY-6, like ADR1 (Parrada et al., 1988) and Xfin-31 (Lee et al., 1989) peptides, forms a rigid and well-defined tertiary

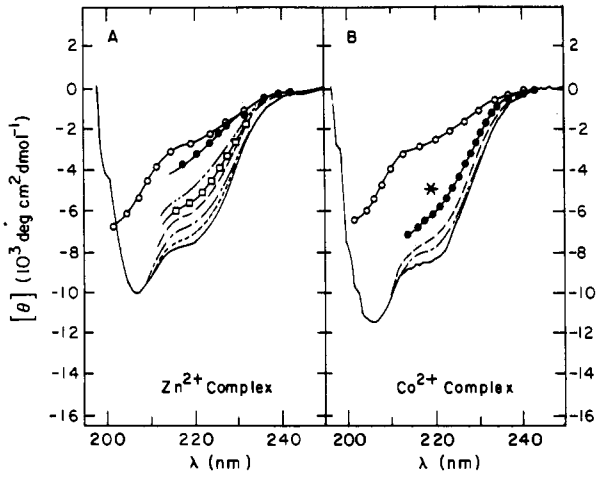

FIGURE 5: Partial unfolding of ZFY-6 in (A) Zn^{2+} complex and (B) Co^{2+} complex as a function of guanidine hydrochloride concentration at 22 °C. Guanidine concentrations: (—) 0 M; (- - -) 0.5 M; (– – –) 1.6 M; (– –) 2.9 M; (□) 3.9 M; (– – – –) 6.2 M; (●) 9 M. CD spectra in the absence of metal are indicated in both panels by open circles (○). Asterisk indicates conditions under which metal binding is retained as indicated by the absorption spectrum of the Co^{2+} complex. The peptide concentration was 113 μM.

structure encaging the metal. Sequential assignment of the NMR spectrum of ZFY-6 and detailed structural analysis will be published separately.

(*d*) *Zn^{2+} affinity* of ZFY-6 may be assessed by competition with known chelators. Successive addition of EDTA is observed to displace Zn^{2+} or Co^{2+} from the finger, resulting in loss of ordered structure (see Figure 6C). Tenfold molar excess EDTA is required to displace >50% Zn^{2+} from the wild-type peptide complex at pH 7.5.

(*e*) *pH Stability.* Co^{2+} absorbance bands exhibit progressive attenuation as the pH is reduced (Figure 2, spectra a–f). This pH behavior presumably reflects protonation of the histidine and/or cysteine ligands and provides a measure of structural stability that may be compared among peptide analogues (Design of Second-Site Revertant). Half-maximal displacement of the native Co^{2+} complex is observed at pH 5.8; the associated α-helical transition, as monitored by CD, exhibits parallel attenuation under acidic conditions (Weiss et al., 1990). Half-maximal displacement of the Zn^{2+} complex occurs at pH 4.5 (not shown). ^{1}H NMR spectra obtained at the midpoint of the pH-unfolding curve demonstrate slow exchange between folded and unfolded species, reflecting a two-state process; such two-state unfolding has also been described in an ADR1 finger (Parraga et al., 1990).

(*f*) *Structural Stability.* Partial unfolding of the Zn^{2+}/peptide complex is observed with successive addition of guanadine hydrochloride at pH 7.5. Such unfolding provides an additional measure of structural stability that may be compared among analogues (Design of Second-Site Revertant). Surprisingly, even in saturated guanidine solutions, metal binding is retained by the native peptide, as indicated by observation of Co^{2+} d–d bands in the visible absorption spectrum (not shown). The peptide retains significant ordered structure under these conditions, as indicated by partial retention of α-helical CD bands (Figure 5). Interestingly, the Zn^{2+} complex (panel A) exhibits less ordered structure in 9 M guanidine hydrochloride than does the Co^{2+} complex (panel B).

Design of Second-Site Revertant. Four analogues of ZFY-6 were designed to evaluate the structural role of the central aromatic residue (Y10) and the implications of its alternative positioning in odd and even ZFY domains. Characterization

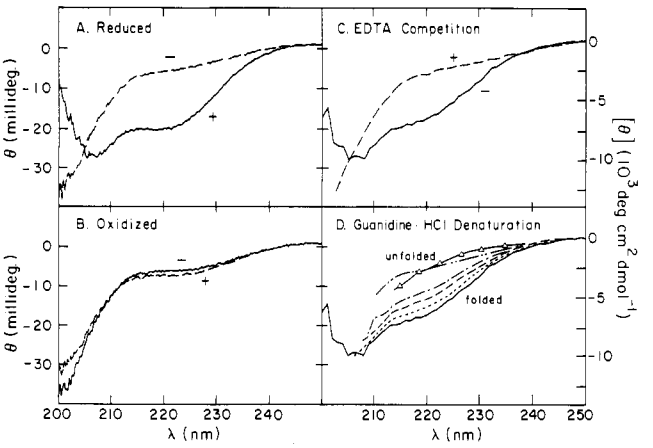

FIGURE 6: Representative CD spectra of ZFY-6[Y10K]: (A) spectrum of the reduced analogue in the absence (labeled –) and presence (labeled +) of equimolar Zn^{2+}; (B) spectrum of the oxidized analogue (i.e., containing an intramolecular disulfide) in the absence (labeled –) and presence (labeled +) of equimolar Zn^{2+}; (C) complete displacement of Zn^{2+} from the reduced complex observed with equimolar EDTA (spectrum of the intact Zn^{2+} complex is labeled –, and spectrum of the EDTA-dissociated peptide is labeled +); (D) unfolding in guanidine hydrochloride. The following concentrations were used: (—) 0 M; (- - -) 1.8 M; (– –) 3.1 M; (– – –) 4.5 M; (△) 9 M. A control spectrum in the absence of divalent metal is shown (– – – –). No Co^{2+} binding is detected in the absorption spectrum in 9 M guanidine hydrochloride. Conditions: 90 μM peptide concentration at 22 °C and pH 7.5.

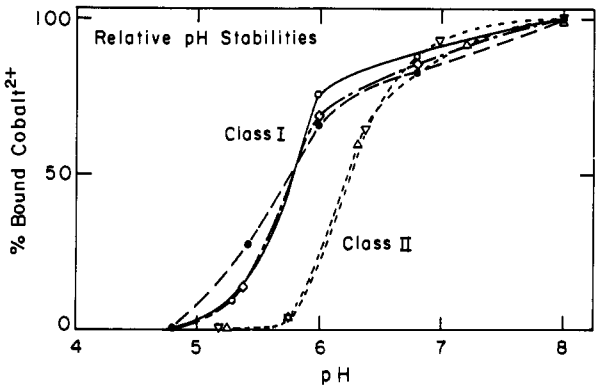

FIGURE 7: Relative pH stabilities of wild-type and mutant Co^{2+} complexes. Class I fingers: wildtype (○), aromatic swap analogue [Y10K; S12F] (◇), and doubly aromatic analogue S12F (●). Class II fingers: Y10K (▽) and Y10S (△). Percent bound Co^{2+} was monitored by amplitude of d–d absorption bands (Figure 2). pH midpoints are given in Table II.

Table II: Relative pH Stabilities[a] of the Co^{2+}–Peptide Complexes

peptide	pH midpoint	peptide	pH midpoint
ZFY-6	5.8	ZFY-6[S12F]	5.7
ZFY-6[Y10S]	6.25	ZFY-6[Y10K; S12F]	5.8
ZFY-6[Y10K]	6.25		

of the parent peptide (see Characterization of ZFY-6) provides a foundation for comparative study of these analogues. Each of the mutations studied (Y10S, Y10K, K12F, and Y10K;-K12F; see Table I and Figure 1A) permits specific tetrahedral coordination of Co^{2+}, as indicated by identical visible absorption spectra (not shown). Representative CD data for one of the analogues (Y10K) are shown in Figure 6. Metal-dependent folding of the reduced peptide and an oxidized control is shown in panels A and B, respectively; displacement of Zn^{2+} by EDTA competition is shown in panel C; and progressive unfolding with guanidine hydrochloride is shown in panel D. The relative stabilities of the four analogues to denaturation

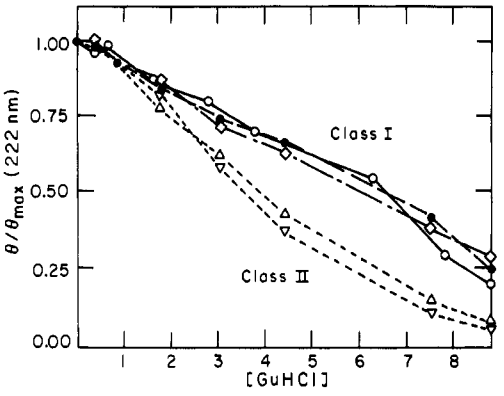

FIGURE 8: Relative structural stabilities of wild-type and mutant Zn^{2+} complexes in guanidine hydrochloride. Class I fingers: wildtype (○), aromatic swap analogue [Y10K; S12F] (◇), and doubly aromatic analogue S12F (●). Class II fingers: Y10K (▽) and Y10S (△).

under acidic conditions are shown in Figure 7 and Table II; relative sensitivities to guanidine hydrochloride are shown in Figure 8.

(*a*) *Mutation of Y10 Destabilizes the Zinc Finger.* CD spectra of the ZFY-6[Y10K] and ZFY-6[Y10S] Zn^{2+} complexes, shown in Figure 3A (spectra a and b, respectively), are similar to the spectrum of the parent peptide (spectrum c). Thus, nonaromatic substitutions at position Y10 are surprisingly well tolerated under native conditions. ZFY-6[Y10S] and ZFY-[Y10K] Zn^{2+} complexes are, however, less stable than that of the native peptide, as indicated by their relative pH stabilities (designated class II in Figure 7). In addition, these analogues (class II in Figure 8) are more sensitive to guanidine than the native peptide (class I). Relative Zn^{2+} affinities are also reduced: whereas for the native finger a 10-fold excess of EDTA is required at pH 7.5 for half-maximal displacement of Zn^{2+}, the Y10K and Y10S analogues are fully unfolded in equimolar EDTA (Figure 7C). Although it will be important in future studies to extend these observations to nonaromatic hydrophobic residues (e.g., leucine) at positions 10 and 12, the present results demonstrate a coupling between metal binding and loop sequence mediated by stabilization of tertiary structure. Such a coupling has previously been inferred from genetic studies of zinc-supressible *Gal4* mutations in *Saccharomyces cerevisiae* (Johnston, 1987).

(*b*) *Design of a Second-Site Revertant.* The odd-numbered domains follow a consensus K10–F12 pattern, in accord with the general Zn finger consensus. Supposing that Y10-S12 and K10-F10 provide alternative packing motifs, we predicted that an aromatic swap second-site mutation, S12F, would structurally revert the instability of ZFY-6[Y10K]. This is indeed the case (class I in Figures 7 and 8). The CD spectrum of the second-site revertant (spectrum d in Figure 3B) is similar to that of ZFY-6 (spectrum c), although it exhibits somewhat less α-helix.

(*c*) *Analogue Containing Two Aromatic Residues.* The CD spectrum of ZFY-6[S12F] (spectrum e in Figure 3B) indicates partial loss of helical structure relative to ZFY-6 (spectrum c) or ZFY-6[Y10K; S12F] (spectrum d). It is possible that to accommodate the packing of both aromatic rings a perturbation is transmitted (via the hydrophobic core) to the C-terminal helix. This spectroscopic perturbation is partially reverted by the second-site mutation Y10K (analogue [Y10K; S12F]; spectrum d). Aromatic contributions may also occur in this region of the CD spectrum and account in part for differences among analogues; accordingly, detailed structural interpretation will require comparative 2D NMR or crystallographic studies. Surprisingly, ZFY-6[S12F] is as stable as the native peptide (class I in Figures 7 and 8).

Discussion

Two-dimensional NMR studies have been conducted of single-finger peptides from *Saccharomyces* protein ADR1 and *Xenopus* protein Xfin (Parraga et al., 1988; Lee et al., 1990). These studies demonstrate a compact globular minidomain in which the divalent metal is encaged. The N-terminal portion of the finger, containing the conserved cysteines, forms a β-sheet and turn; the C-terminal portion, containing the conserved histidines, forms an α-helix. These features are in accord with earlier structural models (Berg, 1988; Gibson et al., 1988). However, the two NMR structures appear to differ in important respects, and the origins, generality, and functional implications of these differences are not presently understood. Are there general rules that regulate metal-dependent folding? Recent studies of peptide analogues of the ADR1 fingers (Parrage et al., 1990) indicate that thiol and imidazole participation in zinc binding (with proper spacing) are specific requirements for proper folding of the finger motif. These results are extended in the present work to examine the informational content of conserved "framework" residues in the hydrophobic core.

The ZFY gene family—encoding a subgroup of Zn finger proteins distinguishable by a two-finger repeat—provides a model system for studying sequence-dependent variations in finger architecture. Odd-numbered domains resemble the general Zn finger consensus, whereas even-numbered fingers show systematic differences (Page et al., 1987). Because these differences have been strictly conserved among vertebrates, they are likely to identify positions of high informational content. We have recently shown that odd and even ZFY domains exhibit similar but not identical patterns of metal-dependent folding as monitored by circular dichroism (Weiss et al., 1990).

In this paper we have explored the structural meaning of one aspect of the two-finger repeat—the alternative position of the central aromatic residue—in a peptide model of an even-numbered domain (domain 6 in the human ZFY sequence; residues 161–191 of the putative DNA-binding domain). Analogues lacking the central aromatic residue exhibit metal-dependent folding, and their CD spectra are similar to that of the native peptide. Accordingly, a finger template that requires a central aromatic residue (Frankel & Pabo, 1988) is too restrictive, since native architecture is compatible with nonaromatic substitutions. Nevertheless, "zinc fingers" remain distinguishable from general metal-binding loops and as such are likely to be governed by a specific set of "folding rules".

To deduce these rules, we have examined the solution structure and stability of a series of analogues. The successful design of ZFY-6[Y10K; S12F] as a second-site revertant suggests that alternative aromatic rings at positions i and $i + 2$ of a β-sheet can occupy similar spatial positions (Berg, 1988), as illustrated in schematic form in panels B–D of Figure 1. From the perspective of the aromatic ring, this model elegantly viewed the remaining peptide as alternative ring substituents in a (1,4) switch (Berg, 1988). The general features of this model have been verified by 2D NMR studies of single Zn fingers (Parraga et al., 1988, 1990; Lee et al., 1989): positions 10 and 12 (using the ZFY-6 numbering scheme; Figure 1A) indeed form part of a β-strand, and the central aromatic residue (F12) packs against the conserved leucine and the N-terminal histidine. However, it is possible that Y10 and F12 may occupy different sites yet stabilize tertiary structure via complementary but structurally inequivalent interactions. Distinguishing between these possibilities will require com-

parative structural characterization of a series of related analogues by 2D NMR or X-ray crystallography.

Conclusions

The two-finger repeat observed in the ZFY-related gene family provides a foundation for rational protein design. Substitution of the conserved central aromatic residue by nonaromatic amino acids destabilizes the Zn finger; stability is restored in an aromatic swap revertant containing an aromatic residue at an alternative site. The present study thus demonstrates that alternative aromatic positions 10 and 12 provide complementary interactions within the *Cys-X_2-Cys/His-X_4-His* metal-binding motif. Additional architectural rules may be explored by mutagenesis as a general model for metal-dependent protein folding.

Acknowledgments

We thank M. Kochoyan and Q. X. Hua for assistance with NMR assignment and K. A. Mason for technical assistance; C. A. Dahl for advice regarding peptide synthesis; D. C. Page and P. A. Sharp for helpful discussion and communication of results prior to publication; S. Lehrer (Boston Biomedical Research Institute and Harvard Medical School, Boston, MA) for use of a CD spectropolarimeter; D. Case and P. E. Wright for the coordinates of Xfin-31 and helpful discussion; and C. T. Walsh for a critical reading of the manuscript. M.A.W. is supported in part by the Pfizer Scholars Program for New Faculty.

References

Barany, G., & Merrifield, R. B. (1979) in *The Peptides* (Gross, E., & Meienhofer, J., Eds.) Vol. 2, pp 1–284, Academic Press, New York.

Berg, J. M. (1987) *Science 232*, 485–488.

Berg, J. M. (1988) *Proc. Natl. Acad. Sci. U.S.A. 85*, 99–487.

Bull, J. J., Hillis, D. M., & O'Steen, S. (1988) *Science 242*, 567–569.

de la Chapelle, A. (1972) *Am. J. Hum. Genet. 24*, 71–105.

Diakun, G. P., Fairall, L., & Klug, A. (1986) *Nature 324*, 698–699.

DiLella, A. G., Page, D. C., & Smith, R. G. (1990) *New Biol. 2*, 49–55.

Evans, R. M., & Hollenberg, S. M. (1988) *Cell 52*, 1–3.

Fan, C.-M., & Maniatis, T. (1990) *Genes Dev. 4*, 29–42.

Frankel, A. D., & Pabo, C. O. (1988) *Cell 55*, 675–676.

Frankel, A. D., Berg, J. M., & Pabo, C. O. (1987) *Proc. Natl. Acad. Sci. U.S.A. 84*, 4841–4845.

Gibson, T. J., Postma, J. P. M., Brown, R. S., & Argos, P. (1988) *Protein Eng. 2*, 209–218.

Hope, I., & Struhl, K. (1986) *Cell 46*, 885–894.

Johnston, M. (1987) *Nature 328*, 353–355.

Klug, A., & Rhodes, D. (1987) *Trends Biochem. Sci. 12*, 464–468.

Koopman, P., Gubbay, J., Colignon, J., & Lovell-Badge, R. (1989) *Nature 342*, 940–942.

Lee, M. S., Gippert, G. P., Soman, K. V., Case, D. A., & Wright, P. E. (1989) *Science 245*, 635–637.

Ma, J., & Ptashne, M. (1987) *Cell 51*, 113–119.

Maekawa, T., Sakura, H., Sudo, T., & Ishii, S. (1989) *J. Biol. Chem. 264*, 14591–14593.

Mardon, G., & Page, D. C. (1989) *Cell 56*, 765–770.

Mardon, G., Mosher, R., Disteche, C. M., Nishioka, Y., McLaren, A., & Page, D. C. (1989) *Science 243*, 78–243.

Mardon, G., Luoh, S.-W., Simpson, E. M., Gill, G., Brown, L. G., & Page, D. C. (1990) *Mol. Cell. Biol. 10*, 681–688.

Nagamine, C. M., Chan, K., Hake, L. E., & Lau, Y.-F. C. (1990) *Genes Dev. 4*, 63–74.

Nietfeld, W., El-Baradi, T., Mentzel, H., Pieler, T., Koster, M., Poting, A., & Knochel, W. (1989) *J. Mol. Biol. 208*, 639–659.

Page, D. C., Brown, L. G., & de la Chapelle, A. (1987a) *Nature 328*, 437–440.

Page, D. C., Mosher, R., Simpson, E., Fisher, E. M. C., Mardon, G., Pollack, J., McGillivray, B., de la Chapelle, A., & Brown, L. G. (1987b) *Cell 51*, 1091–1104.

Palmer, M. S., Sinclair, A. H., Berta, P., Ellis, N. A., Goodfellow, P. N., Abbas, N. E., & Fellous, M. (1989) *Nature 342*, 937–939.

Parraga, G., Horvath, S. J., Eisen, A., Taylor, W. E., Hood, L., Young, E. T., & Klevit, R. E. (1988) *Science 241*, 1489–1492.

Parraga, G., Horvath, S., Hood, L., Young, E. T., & Klevit, R. E. (1990) *Proc. Natl. Acad. Sci. U.S.A. 87*, 137–141.

Schneider-Gadicke, A., Beer-Romero, P., Brown, L. G., Nussbaum, R., & Page, D. C. (1989) *Cell 57*, 1247–1258.

Sinclair, A. H., Foster, J. W., Spencer, J. A., Page, D. C., Palmer, M., Goodfellow, P. N., & Graves, J. A. (1988) *Nature 336*, 780–783.

Stewart, J. M., & Young, J. D. (1984) *Solid Phase Peptide Synthesis*, Raven Press: New York.

Tregear, G. W., van Reitschoten, J., Sauer, R. T., Niall, H. D., Keutmann, H. T., & Potts, J. T. (1977) *Biochemistry 16*, 2817–2823.

Weiss, M. A., Mason, K. A., Dahl, C. E., & Keutmann, H. T. (1990) *Biochemistry 29*, 5660–5664.